

RSC Advances



This article can be cited before page numbers have been issued, to do this please use: H. Xie, T. Lin, L. Shi and X. Meng, *RSC Adv.*, 2016, DOI: 10.1039/C6RA17567H.



This is an *Accepted Manuscript*, which has been through the Royal Society of Chemistry peer review process and has been accepted for publication.

Accepted Manuscripts are published online shortly after acceptance, before technical editing, formatting and proof reading. Using this free service, authors can make their results available to the community, in citable form, before we publish the edited article. This *Accepted Manuscript* will be replaced by the edited, formatted and paginated article as soon as this is available.

You can find more information about *Accepted Manuscripts* in the [Information for Authors](#).

Please note that technical editing may introduce minor changes to the text and/or graphics, which may alter content. The journal's standard [Terms & Conditions](#) and the [Ethical guidelines](#) still apply. In no event shall the Royal Society of Chemistry be held responsible for any errors or omissions in this *Accepted Manuscript* or any consequences arising from the use of any information it contains.

Acetylene carbonylation over Ni-Containing Catalysts: Role of Texture and Active Site Distribution

Hao Xie, Tiejun Lin, Li Shi, Xuan Meng*

The State Key Laboratory of Chemical Engineering, East China University of Science and Technology, Shanghai 200237, People's Republic of China

Abstract

Heterogenization of homogeneous catalyst for acetylene carbonylation was carried out by preparing a series of Ni modified catalyst (Ni-ZSM-5, Ni-IM-5 and Ni-MCM-41). Several important properties of heterogeneous catalyst were determined by ICP-AES, XPS, XRD, N₂ adsorption, pyridine-FTIR, SEM and TGA. Moreover, we using various activity criterion to dissipate the disturbed factors, when we focus on the influence of texture and active site distribution. The result that Ni-IM-5 had the greatest TOF_{Ni}=5107 g acrylic acid/ (g Ni·h), showed that the texture of samples did not influence the catalyst performance significantly. And the highest ratio of nickel site/acid site in Ni-MCM-41 represented the best active site distribution. Thus, Ni-MCM-41 have the highest TOF_{Cat.}=70.6 g acrylic acid/ (g cat.·h). Furthermore, the stability test of catalyst showed the Ni-MCM-41 could use four times, while others only twice.

Keywords: Carbonylation, Acetylene, Molecular sieve, Acid site, Texture

* To whom correspondence should be addressed. E-mail: mengxuan@ecust.edu.cn
Tel.: 021-64252383.

1 Introduction

Unstable supplement and volatility price of oil, make the acetylene had received renewed attention, recently^[1]. Because of thermodynamic active state and broader sources (like natural gas, coal or shale gas) of feedstock, acetylene-based process become the potential route for alternating petroleum to manufacture bulk chemicals, like acrylic acid^[2-3]. Generally, nickel-based catalysts, especially the Ni(CO)₄ and the nickel halide, are commonly used as active homogeneous catalysts for acetylene carbonylation to gain acrylic acid (Scheme 1)^[4-7]. According to these reports, no matter using the toxic catalyst Ni(CO)₄ or the nickel halide, the highest acrylic acid are the same, ~70%. Otherwise, except the danger of toxicity, it is difficult to separate the production and the homogeneous catalyst.

With respect to the green chemistry principles, heterogenization of homogeneous catalyst for acetylene carbonylation have become one of the most attractive areas^[8, 9]. The team of Bhattacharyya had investigated the reaction carried out on Ni complex-silica, in 1960s^[6, 10-11]. However, the catalyst performance is not as good as expectation. In their reports, the highest conversion of acetylene is just 8.56%, means that all of these investigated heterogeneous catalyst was little active for this reaction. Molecular sieves are one of the most commonly used heterogeneous catalysts for many reactions^[12]. Sarkar B R^[13] et al use the MCM-41 as the support to promote the catalyst activity. Modified ZSM-5^[14] also have been considered as an efficient heterogeneous catalysts for the carbonylation. In general, the activity of transition metal-containing zeolites relies on the containing of metal and on the nature of the

zeolite with respect to the strength and concentration of acid sites, pore dimensions, and accessibility of acid sites. Therefore, the difference in activity between different molecular sieves should be more pronounced, especially in the condition that the heterogeneous catalyst for acetylene carbonylation needs more fundamental research.

We have already reported catalyst NiY (prepared by ion-exchange) performed better than NiO-Y (prepared by impregnation) in acetylene carbonylation^[16]. More property of Ni-exchanged molecular sieves, such as texture and active site, would be investigated in this context. Nickel modified various molecular sieves (ZSM-5, IM-5 and MCM-41) was synthesized via ion-exchanged. Active metal content and state were determined by ICP-AES and XPS, while structural information was obtained through XRD and N₂ adsorption, and acidity property was measured by FT-IR using pyridine probe. As for the surface photographs of fresh and recovered catalysts were taken by SEM. Our attention has also focused on the reusable of catalysts.

2. Experimental

2.1. Catalyst preparation.

The raw materials were either purchased (ZSM-5, IM-5) or home-synthesized (MCM-41). Zeolite NaZSM-5 ($\text{SiO}_2/\text{Al}_2\text{O}_3 = 50$, Nankai University catalyst Co., Ltd.) and NaIM-5 ($\text{SiO}_2/\text{Al}_2\text{O}_3 = 48$, Institute of Petrochemical Research) were used as received and in powder form. MCM-41 was synthesized using the method reported by Zhao X S^[17]. A precursor gel was composed of fumed silica, sodium silicate ($\text{Na}_2\text{SiO}_3 \cdot 9\text{H}_2\text{O}$), cetyltrimethyl ammonium bromide (CTAB), deionized water and concentrated sulfuric acid (H_2SO_4) with the molar composition of 1.0 SiO_2 :0.2 CTAB:60 H_2O . The precursor solution stirred for 2 h at room temperature followed by crystallization in a Teflon-lined autoclave at 120°C for 2 days under autogenous pressure. The solids were recovered by filtration, washed with deionized water, and dried at 120°C overnight. And heated to 550°C at a heating rate of 2°C/min and calcined at 550°C for 6 h to remove the template.

All the parent materials were prepared by ion-exchanged procedure to introduce nickel ion. For ion-exchanged process, 1g of molecular sieve was exchanged with 20 mL of 100 mM/L $\text{Ni}(\text{NO}_3)_2$ solution, under the condition that at 363 K and stirring for 24 h in a round-bottomed flask followed by filtration, washed thoroughly using deionized water, dried at 120°C for 12 h. Then transferred into a muffle furnace, and calcined at 550°C for 5 h in static air atmosphere. The resulting samples denoted as Ni-X (X= ZSM-5, IM-5, MCM-41).

2.2. Catalyst activity.

The catalytic carbonylation of acetylene was carried out in a 0.5 L stainless steel-316 Parr autoclave having the gas inlet and outlet, a rupture disk for safety measure, intermediate sampling, temperature-controlled heating, and variable agitation paddle. In a typical experiment, known quantities of catalyst powders (0.5 g), promoters (0.2077 g CuBr₂), H₂O (15 ml), and acetone (150 mL) were added into a stirred pressure reactor which inflated with nitrogen several times for purification and subsequently pressurized with acetylene to 0.4 MPa and then to 4.0 MPa of initial total pressure with CO (both controlled by mass flowmeter and the molar ratio of CO/C₂H₂=1.05) at room temperature. After reaction completed at 235°C and stirring rate was 200 rpm, the autoclave was quickly cooled to room temperature and the tail gas and liquid were collected, calculated and analyzed. The detailed schematic drawing of the reactor can be found elsewhere^[18]. The conversion of acetylene, selectivity and yield of acrylic acid and the turnover of frequency (TOF) are defined as follows:

$$Yield = \frac{n_p}{n_0} \times 100\% \quad (\text{Eq. 1})$$

$$TOF_{Cat.} = \frac{g_{AA}}{g_{cat} \cdot h} \times 100\% \quad (\text{Eq. 2})$$

$$TOF_{Ni} = \frac{g_{AA}}{g_{Ni} \cdot h} \times 100\% \quad (\text{Eq. 3})$$

Where,

n_0 , molar content of acetylene for feedstock before reaction;

n_p , molar content of acetylene for forming acrylic acid;

g_{AA} , the mass of acrylic acid produced during reaction;

g_{cat} , the mass of catalysts for input before reaction;

g_{Ni} , the mass of nickel contained in the catalysts for input before reaction.

2.3. Characterization

The samples were previously dissolved by acid digestion followed by measured by inductively coupled plasma atomic emission spectroscopy (ICP-AES, Varian 710ES). And Chemical composition in prepared catalyst was determined.

The chemical state of nickel ion on the catalyst was obtained, by XPS using a Perkin–Elmer PHI 5000 C ESCA system equipped with Mg anode. Their binding energies were corrected by the C 1s line at 284.6 eV.

The crystal structure of samples was characterized by X-ray diffractometer (XRD, Bruker D8, Germany) equipped with an atmosphere and temperature control stage and using Cu K α radiation ($\lambda = 1.5406 \text{ \AA}$) operated at 40 kV and 100 mA. The scanning range from 10 ° to 80 ° (2θ), 0.02 step, and 1 s/step.

The texture porosity of the samples were performed using a Micromeritics ASAP 2010 nitrogen adsorption instrument. All samples were degassed under vacuum at 300°C overnight, prior to measurements. The microporous volume, mesoporous volume and specific surface area of the catalyst were calculated using HK, BJH and BET method.

The acidity property of the samples was determined by Fourier transform infrared (FT-IR) spectroscopy (Nicolet Company, Model Magna-IR550) using pyridine as the probe. Self-supported wafers previously saturation adsorption of pyridine at 80°C followed by cooling to ambient and under vacuum of 10^{-2} Pa for 90

min. Afterwards, total acid sites (T) of sample were measured after desorption at 200°C. The pyridine adsorption, measured after desorption at 450°C, represents the strong acid sites (S). The difference represents the weak acid sites (W). There are two varieties of acid: one is a Brønsted acid (denoted as B), whose characteristic absorption peak is located at 1545 cm⁻¹; and the other is a Lewis acid (denoted as L), located at 1450 cm⁻¹. And Lewis and Brønsted acidic site can be calculated via the Lambert–Beer law: $A = \xi \cdot C \cdot d$ where A is absorbance, C is sample concentration, ξ is extinction coefficient and d is sample thickness. Surface acid contents of adsorbents for Lewis acid and Brønsted acid were calculated by using empirical formulas which are obtained from the relevant experiments.

$$C_L (\text{mol} \cdot \text{g}^{-1}) = 3.73 \times 10^{-3} A_L \quad (\text{Eq. 4})$$

$$C_B (\text{mol} \cdot \text{g}^{-1}) = 9.90 \times 10^{-3} A_B \quad (\text{Eq. 5})$$

Where C_L and C_B are respectively Lewis and Brønsted acid contents (mol g⁻¹), A_L and A_B are respectively peak areas in 1450 cm⁻¹ (denoted as L) and in 1545 cm⁻¹ (denoted as B)^[19, 20].

The morphologies of fresh and recovered catalysts were obtained using a Nova Nano SEM450.

The recovered catalysts were measured by thermo-gravimetric analysis (TGA). The samples were heated up to 800°C at 10°C/min under flowing air at 100 ml/min, recording continuously the weight of each sample.

3. Result and discussion

3.1. Component analysis

The chemical elements of parent material and Ni-modified catalyst were determined by ICP-AES. The Ni loading, charge balanced of Na and Ni, and the ratio of silicon to aluminum are present in Table 1. As we can see, all the raw material has the similar Na Content (1.5/1.4/1.9 wt. % on ZSM-5, IM-5 and MCM-41). Otherwise, Ni-MCM-41 has the highest Ni loading, 2.08 wt. % while the Ni-ZSM-5 and Ni-IM-5 are 1.51 %, 1.27 %, respectively. Valent analysis of nickel on the reaction was measured by XPS, and the results are presented in Fig. S1. Ni 2p_{3/2} region shows two main components peak maxima with binding energies of ~856.1 and ~861.9 eV. The appearance of these two peaks indicating the existence of divalent nickel and its complex multiple species (not including Ni oxides), respectively^[21, 22]. Oliveira et al^[23] interpreted the behavior of the Ni 2p_{3/2}, and regarded that the characteristics peaks at ~856.0 were assigned to Ni²⁺. Even though these two peaks' positions of Ni-modified catalysts was little different, it could be contributed to the measured error. Because of the same modification, including the preparation method and the treated condition, the valence state of nickel was the same, even it supported on different molecular sieves^[24, 25].

3.2. Structure characterization

The XRD patterns of parent materials and the corresponding modified catalyst are presented in Fig. S2. The patterns of the non-exchanged molecular sieve correspond well to those reported in the literatures as well as the modified samples^{[17,}

^{26]}. Compared to the parent materials, there is no significant structural modification and none of nickel oxide after nickel modified was found in the XRD patterns. According to the literature, the metal cations introduced to the molecular sieves by ion-exchange process are in the form of a skeleton balance-charge. It means that one Ni^{2+} cation exchanged into the zeolite charges compensate two charge sites (Na). Thus value of $n(2\text{Ni} + \text{Na})$ in catalyst should be equal to $n(\text{Al})$ and original $n(\text{Na})$, namely their ratios should be a constant value (≈ 1.0)^[20]. From the Table 1, it is easy to conclude that the nickel cations compensated to the skeleton structure and exist as charge-compensating as well as highly dispersed^[27]. Furthermore, the color of samples prepared via incipient wetness impregnation (IWI, 2 wt. %) is gray, which is much more different from the white Ni exchanged catalysts (Fig. S3). In the patterns of XPS, it is also hard to find the characteristic peaks of Ni oxides. And the X-ray diffraction peaks of the modified samples were less intense, indicated the slight decrease in the crystallinities of sample during the introduction process of metal ions and subsequent calcination.

Textural properties of catalysts are given by N_2 adsorption-desorption isotherms and showed in Fig. 1. Due to little uptake of nitrogen, an almost horizontal isotherm was found at the P/P_0 range from 0.1 to 0.4 for Ni-exchanged ZSM-5 and IM-5. It reflected the presence of micropores^[28]. When nitrogen desorbed at P/P_0 higher than 0.4, hysteresis loops in the desorption branch were observed, which indicated the presence of mesopores in Ni-ZSM-5 and Ni-IM-5. The isotherm of Ni-ZSM-5 and Ni-IM-5 was type IV and type I, respectively. As for Ni-MCM-41, due to the

characteristic capillary condensation within mesopores and multilayer adsorption on the outer surface, it exhibits a type IV nitrogen adsorption-desorption isotherm^[29, 30]. Moreover this isotherm was likely the combination of the shapes of type I and type IV in the range P/P_0 more than 0.4. It meant the Ni-MCM-41 contained the features of mesoporous properties of the samples above.

Table 2 shows the calculated texture properties of different Ni-modified catalysts, including specific surface area (S), micropore and mesopore volumes (V_{micro} , V_{meso}). Because of the same MFI structure, Ni-ZSM-5 and Ni-IM-5 have the similar specific surface area and microporous volume. These results agree with the previously reported data^[31,32]. Significant mesoporous volumes and a high adsorption corresponding to the presence of pores with diameters in the range of large mesoporosity were observed in Ni-IM-5 and Ni-MCM-41(Fig. 1). Table 2 shows that the Ni-MCM-41 has the largest specific surface area, more than 1300 m²/g, as well as the largest mesoporous volume.

3.3. Acidity determination

In order to investigate the relationship between reaction performances and the properties of acidic sites on the catalyst, the spectra of FT-IR using pyridine as the probe molecule was obtained and shown in Fig. 3. At 200°C, the vibrations of pyridine molecules bound at 1450 cm⁻¹ was stronger than the peaks centered at 1545 cm⁻¹ for all the samples. It suggested that the total L acid site was more abundant than B acid site on all Ni-modified samples. And all of the zeolites have the obvious characteristic peaks at 1490 cm⁻¹, arising due to overlaps of $\nu(\text{C}-\text{C})$ vibration of

pyridine adsorbed at L and B acid site. After the samples treated at 450°C, all the peaks appeared at 200°C became almost invisible, especially for the spectrum of Ni-ZSM-5 and Ni-IM-5, meant the less strong acid site. The more detail important features were obtained by the Equation (4) and (5), and showed in Table 3. The weak acid site on almost all samples are dominated. Meanwhile, L acid site was richer than B acid site, no matter weak or strong acid site. However, there was several difference among them. L and B acid site on Ni-ZSM-5 was relatively balanced, while Ni-MCM-41 have much more L acid site than B acid site, no matter the strong or weak acid site. As for Ni-IM-5, the amount of strong B is more than strong L acid site and weak acid site distribution is relatively balanced.

3.2. Catalytic activity

The different Ni-exchanged samples were tested by acetylene carbonylation. The reaction was carried out in the autoclave at the temperature 235°C and 4 MPa of initial total pressure for 120 min. Catalytic evaluation using parent materials (ZSM-5, IM-5 and MCM-41) was also performed, and no acrylic acid products were obtained in these cases, suggesting that the acid sites alone are not able to activate the reaction under the reaction condition. On the contrary, all the Ni-modified catalysts showed good performance for the acetylene carbonylation, and released that nickel is indispensable. Similarly, Huang et al^[33] regards the nickel as the key to the hydroesterification of acetylene with CO and methyl formate to gain methyl acrylate carbonylation.

Ni-MCM-41 has the greatest TOF_{Cat} , 70.60 g acrylic acid/ (g cat.·h), and TOF_{Cat}

of other two zeolites is 64.50 and 66.40 g acrylic acid/ (g cat. ·h), for Ni-ZSM-5 and Ni-IM-5 respectively. The tendency of $\text{TOF}_{\text{Cat.}}$ is the same as yield, while TOF_{Ni} had something different. Ni-IM-5 have the highest TOF_{Ni} , followed by Ni-ZSM-5 and Ni-MCM-41. The order catalyst activity was different when using different criterion, due to the different factors considered. If used $\text{TOF}_{\text{Cat.}}$, we concentrated on an entire catalyst. While TOF_{Ni} is a helpful standard to dissipate the effect of the number of the metal site. Therefore various TOF were effective in the different situation.

The high nickel-containing Ni-MCM-41 shows the excellent yield for the acetylene carbonylation over other Ni-containing catalysts. However, Ni content in Ni-ZSM-5 is higher than Ni-IM-5, but the yield of Ni-ZSM-5 is weaker than Ni-IM-5. Thus, the amount of nickel is not the only factor influenced the reaction. In order to explain these differences in catalytic activity, other two main categories of properties have to be considered: the textural property and the active site distribution.

In the first case, TOF_{Ni} which assisted to observe the association between catalyst structure and catalyst performance, was selected to present the activity. Related data were showed in Table 2. Focus on the topology and pore architecture of the samples, Ni-ZSM-5 and Ni-IM-5 had the similar microporous texture. The difference in TOF_{Ni} between MFI zeolites might be caused by the mesoporous structure. On the basis of this hypothesis, Ni-MCM-41 which have the mesoporous character of both the MFI zeolites we used, should have the highest TOF_{Ni} . However, hierarchical mesoporous structure might not have the advantage in this reaction, according to the actual TOF_{Ni} . For most of the reaction, when the other factors were similar, a large specific area

means the high performance. Otherwise, Ni-MCM-41 had the largest BET area, but the lowest TOF_{Ni} . While Ni-IM-5 had the second largest BET area, but highest TOF_{Ni} . These results suggesting that the size of the specific area, as well as the pore volume, did not influence the catalyst activity obviously. In a word, topology or pore architecture did not contribute to the reaction activity significantly.

Apart from the molecular sieves structure, active site distribution is the important factor must be concerned. Active site commonly includes the metal site and acid site for metal modified catalyst. Many reactions need acid site to improve the catalyst performance, such as L acid site is helpful for the hydrogenation process. It is generally known that introduced metal into molecular sieve gave rise to new acid sites [34]. This suggesting that metal site played the role of both active site and acid site. For acetylene carbonylation, active intermediates generated on the acid site firstly, and transformed to production on metal site Ni^{2+} [16]. Thus, when considerate the influence of the active site, nickel loading or acid property cannot be explored independently. The ratio of metal site and acid site, presented as value R, is put forward to measure the influence of catalytic sites distribution for reaction quantitatively. The catalyst performance represented as TOF_{Ni} , has removed the Ni containing disturbance. In this section, TOF_{Cat} is used as the criterion for catalyst activity, due to the significant influence of nickel on acid property. And the relevant data is shown in the Table 4. Consequently, R of modified samples followed the order of Ni-MCM41> Ni-IM-5>Ni-ZSM-5, and it met the order of catalyst activity well. Several conclusions were pointed out. Firstly, all the R values are smaller than one, meant all the nickel

played as both acid site and the active site and the support also provided the acid site.

Furthermore, R reflected the rich level of nickel in unit acid site. When intermediates formed on acid site, only a metal site nearby, can the product obtained (Scheme 2).

Therefore, higher the R, better the catalyst performance.

3.2. Catalyst Stability

Reusability is crucial for heterogeneous catalysts and further applications in industrial scale. It is available regarding the stability and recyclability of molecular sieves catalysts in liquid-phase of acetylene carbonylation. Fig. 4 gives the reusability test of Ni modified catalysts for several repeated run. All the tests were carried out at the same initial condition for 120min, except using different kinds of catalysts. It lost more than 50% of initial performance when used Ni-ZSM-5 and Ni-IM-5 catalysts one more time. As for Ni-MCM-41, it lost its 50% of initial activity after the third catalytic run.

The Ni containing of used catalysts and liquid products was measured by ICP. The leakage of Ni happened, but the amount of missing was only ~2.3%, which could be negligible. Furthermore, nickel was hardly detected in the liquid product. Thus, the leakage cannot be the key to the deactivated catalyst. The observation of a small amount of black particles in the recovered catalyst, can be inferred to the coke deposited over the external surface of zeolite. SEM results of fresh and recovered catalyst are shown in Fig. 5. In the SEM micrograph, Ni-ZSM-5 and Ni-IM-5 zeolites (Fig. 5a, 5c) were prohibited as a long cubical shape crystal, which is similar to other literatures^[35]. Otherwise, the crystal shape of Ni-ZSM-5 and Ni-IM-5 was similar, but

Ni-ZSM-5 was bigger than Ni-IM-5 in size. Fig. 5e shows the typical SEM images of Ni-MCM-41, where crystal particles of near sphere can be consistently seen. However, the agglomerates of small particles is easily noted. It is evident that the catalysts retained their microstructure after reaction. Otherwise, the surfaces of all the recovered catalyst turned rough and covered by a layer of tiny particles. The TGA of recovered catalysts (Fig. 6) also indicated the existence of coke, which is line with the findings in the TG-DTG analysis, and is agreement with the above results of reusability test of catalyst. As the TGA of recovered catalyst showed, the weight loss before 200°C in all of the tested samples is attribute to the vaporization moisture. In the range from 200 to 650°C, about 10 wt. % coke was observed on the quickly deactivated catalysts, Ni-ZSM-5 and Ni-IM-5, while almost no coke on Ni-MCM-41. It can referred that the coke may cover the active site, limit the accession of the reactant molecules and deactivate the catalyst.

4 Conclusion

Different Ni-modified catalysts were examined as a case of highly efficient heterogeneous catalyst for the carbonylation of acetylene with carbon monoxide and water to yield acrylic acid. A careful comparison of catalysts prepared by different supports (ZSM-5, IM-5, and MCM-41) reveals that the Ni-MCM-41 showed the highest $\text{TOF}_{\text{Cat.}}=70.60$ g acrylic acid/ (g cat·h) and Ni-IM-5 had the greatest $\text{TOF}_{\text{Ni}}=5108$ g acrylic acid/ (g Ni·h).

Characterization of ICP-AES, XPS, and XRD indicates the introduced nickel existed as Ni^{2+} , and compensated for the skeleton structure. All the modified catalyst maintain their original structure. Activity criterion TOF_{Cat} showed the structure of the molecular sieve did not contribute to activity obviously. It is found that the balance between acid site and nickel site, played a significant role in determining their activity by TOF_{Cat} . The highest $\text{Ni}^{2+}/\text{Acid}$ sites ratio indicates the Ni and acidic functions were well balanced and performed in the acetylene carbonylation best. Reusability test of Ni-modified catalysts exhibited that the mesoporous materials Ni-MCM-41 has the best anti coke deposition and multi-used property.

5 Acknowledgements

We are grateful for financial support from Young Scientific Talents Sail Plan of Shanghai City [15YF1403000] and Special Fund of Fundamental Research and Exploration [22A201514014].

Reference

- [1] C. Boswell, On-purpose technologies ready to fill propylene gap. *ICIS Chemical Business*, **2012**.
- [2] H. Jüntgen, G. Kölling, W. Peters, Comparison of different routes from coal to chemicals and gasoline. *Proceedings of 11th World Petroleum Congress*, London, Aug. 28-Sept. 2, **1983**.
- [3] ICIS Value Chain: Acrylic acid. *ICIS Chemical Business*, **2014**.
- [4] K. Weissermel, H. J. Arpe, *Industrial Organic Chemistry*; VCH: Weinheim, **1993**; pp 286-287.
- [5] W. Reppe, *Acetylene Chemistry*, Meyer, New York, **1949**.
- [6] S. K. Bhattacharyya, A. K. Sen, *J. Appl. Chem.* **1963**, 13, 498-505.
- [7] C. Tang, Y. Zeng, P. Cao, X. Yang, G. Wang, *Catal. Lett.* **2009**, 129, 189-193.
- [8] C. Tang, P. Cao, Y. Zeng, X. Yang, G. Wang, *Petrochem. Technol.* **2008**, 37, 1089-1094.
- [9] I. T. Trotsuş, T. Zimmermann, F. Schüth, *Chem. Rev.* **2013**, 114, 1761-1782.
- [10] S. K. Bhattacharyya, D. P. Bhattacharyya, *J. Appl. Chem.* **1966**, 16, 18-21.
- [11] S. K. Bhattacharyya, D. P. Bhattacharyya, *J. Appl. Chem.* **1966**, 16, 202-205.
- [12] J. Q. Bond, D. M. Alonso, D. Wang, R. M. West, J. A. Dumesic, *Science*, **2010**, 327, 1110-1114.
- [13] B. R. Sarkar, R. V. Chaudhari, *Catal. Today*, **2012**, 198, 154-173.
- [14] K. Narsimhan, V. K. Michaelis, G. Mathies, W. R. Gunther, R. G. Griffin, Y. Román-Leshkov, *J. Am. Chem. Soc.* **2015**, 137, 1825-1832.

- [15] B. I. Mosqueda-Jiménez, A. Jentys, K. Seshan, J. A. Lercher, *J. Catal.* **2003**, 218, 348-353.
- [16] T. J. Lin, X. Meng, L. Shi, *Appl. Catal. A: General*, **2014**, 485, 163-171.
- [17] X. S. Zhao, G. Q. Lu, G. J. Millar, *Ind. Eng. Chem. Res.* **1996**, 35, 2075-2090.
- [18] T. J. Lin, X. Meng, L. Shi, *Ind. Eng. Chem. Res.* **2013**, 52, 14125-14132.
- [19] C. A. Emeis, *J. Catal.* **1993**, 141, 347-354.
- [20] D. Yi, H. Huang, X. Meng, L. Shi, *Appl. Catal. B: Environ.* **2014**, 148, 377-386.
- [21] D. Karthikeyan, N. Lingappan, B. Sivasankar, N. J. Jabarathinam, *Appl. Catal. A: General*. **2008**, 345, 18-27.
- [22] H. Kuhlenbeck, G. Odörfer, R. Jaeger, G. Illing, M. Menges, T. Mull, H.J. Freund, M. Pöhlchen, V. Staemmler, S. Witzel, C. Scharfschwerdt, K. Wennemann, T. Liedtke, M. Neumann, *Phys. Rev. B*, **1991**, 43, 1969-1986.
- [23] M. C. Oliveira, A. B. do Rego, *J. Alloys Compd.* **2006**, 425, 64-68.
- [24] S. Xiao, Z. Meng, *J. Chem. Soc. Faraday Trans.* **1994**, 90, 2591-2595.
- [25] T. Lehmann, T. Wolff, C. Hamel, P. Veit, B. Garke, A. Seidel-Morgenstern, *Micropor. Mesopor. Mater.* **2012**, 151, 113-125.
- [26] H. Liu, S. Wu, Y. Guo, F. Shang, X. Yu, Y. Ma, C. Xu, J. Guan, Q. Kann, *Fuel*, **2011**, 90, 1515-1521.
- [27] A. J. Hernández-Maldonado, R. T. Yang, *Ind. Eng. Chem. Res.* **2003**, 42, 123-129.
- [28] Z. Qin, B. Shen, Z. Yu, F. Deng, L. Zhao, S. Zhou, D. Yuan, X. Gao, B. Wang, H. Zhao, H. Liu, *J. Catal.* **2013**, 298, 102-111.

- [29] K. S. Sing, *Pure Appl. Chem.* **1985**, 57, 603-619.
- [30] M. J. Souza, A. S. Araujo, A. M. Pedrosa, B. A. Marinkovic, P. M. Jardim, E. Morgado, *Mater. Lett.* **2006**, 60, 2682-2685.
- [31] J. Jae, G. A. Tompsett, A. J. Foster, K. D. Hammond, S. M. Auerbach, R. F. Lobo, G. W. Huber, *J. Catal.* **2011**, 279, 257-268.
- [32] Kalita, P. Gupta, N. M. Kumar, R. *J. Catal.* **2007**, 245, 338-347.
- [33] X. H. Huang, X. G. Yang, J. Q. Zhang, Z. T. Liu, *J. Nat. Gas Chem.* **2001**, 10, 42-50.
- [34] D. Esquivel, A. J. Cruz-Cabeza, C. Jiménez-Sanchidrián, F. J. Romero-Salguero, *Micropor. Mesopor. Mater.* **2013**, 179, 30-39.
- [35] H. Liu, S. Wu, Y. Guo, F. Shang, X. Yu, Y. Ma, C. Xu, J. Guan, Q. Kan, *Fuel*, **2011**, 90, 1515-1521.

Table 1 Elemental analysis of raw materials and nickel modified various molecular sieves

Samples	Raw		Modified			Charged Balanced Calculation	
	Na _R ^a	SiO ₂ /Al ₂ O ₃	Ni	Na _M ^b	Al	Cation/Na _R	Cation/Al
NiZSM-5	1.46	43	1.51	0.27	1.71	1.00	0.98
NiIM-5	1.38	45	1.29	0.41	1.65	1.02	1.01
NiMCM-41	1.93	/	2.08	0.30	/	1.00	/

a, Na_R, means the content of Na in the raw materials

b, Na_M, means the content of Na in the modified catalyst

c, means calculated assuming that every positive charge from the exchanged cations can charge compensate an exchange site, Cation=Na + 2Ni.

Table 2 Texture and activity properties of different Ni-modified catalysts

Catalyst	S (m ² /g)	V _{micro} (cm ³ /g)	V _{mesco} (cm ³ /g)	TOF _{Ni} g _{AA} /g _{Ni} ·h
Ni-ZSM-5	230.54	0.117	0.054	4300
Ni-IM-5	267.29	0.136	0.499	5108
Ni-MCM-41	1312.86	/	1.033	3362

Table 3. Acidic properties of different Ni-modified catalysts (m mol/g).

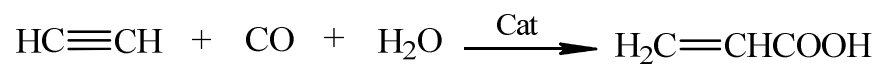
Catalysts	T	T_B	T_L	S_B	S_L	W_B	W_L
Ni-ZSM-5	24.30	11.97	11.33	0.74	0.98	11.23	11.35
Ni-IM-5	17.50	7.06	10.44	0.29	0.02	6.77	10.42
Ni-MCM-41	8.88	1.48	7.40	0.35	1.56	1.13	5.84

T—Total acid; T_L —total Lewis acid; T_B —total Brønsted acid; S_L —strong Lewis acid;

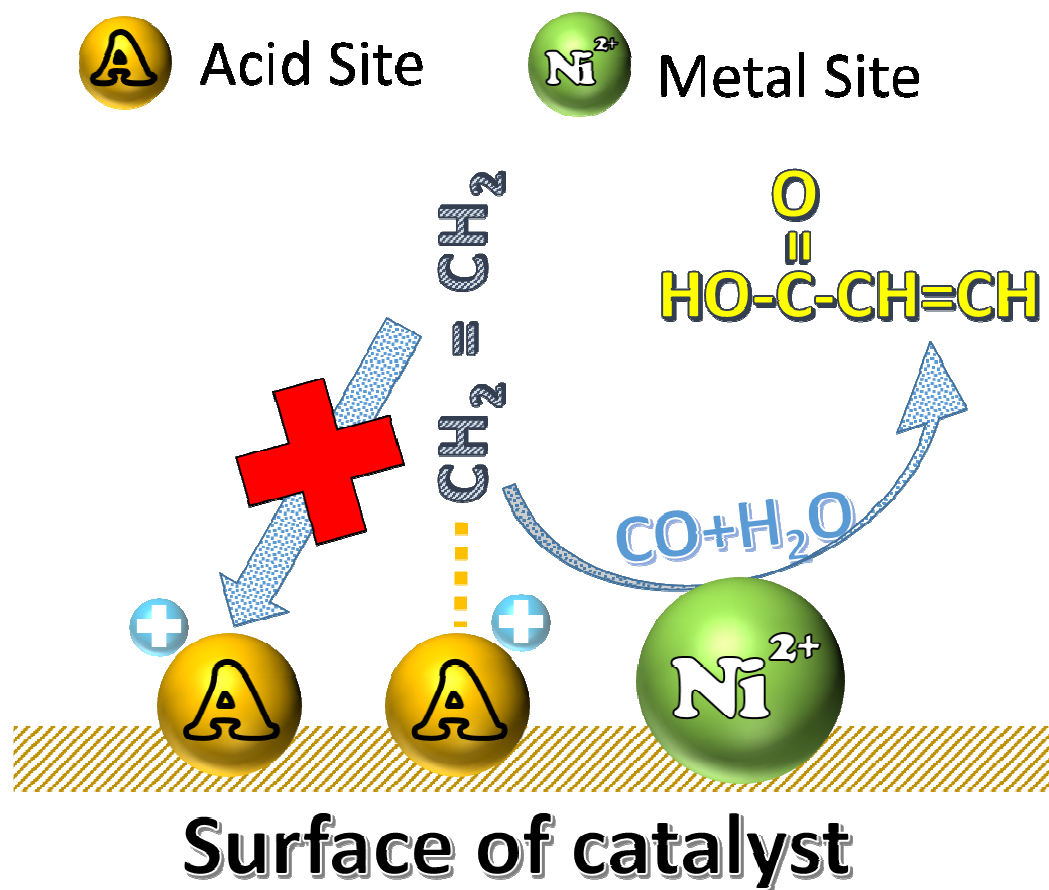
S_B —strong Brønsted acid; W_L —weak Lewis acid; W_B —weak Brønsted acid.

Table 4 Catalytic behavior of different Ni-modified catalysts for acetylene carbonylation

Catalyst	Ni ²⁺	Acid	R(Ni ²⁺ /Acid)	TOF _{Cat.}
	wt, %	m mol/g	mol/ mol	$\frac{g_{AA}}{g_{cat} \cdot h}$
NIZSM-5	1.5	24.30	0.011	64.5
NiIM-5	1.3	17.50	0.013	66.4
NiMCM-41	2.1	8.88	0.040	70.6



Scheme 1. Carbonylation of acetylene with CO and water to yield acrylic acid.



Scheme 2. Active site on the Ni-modified catalyst surface

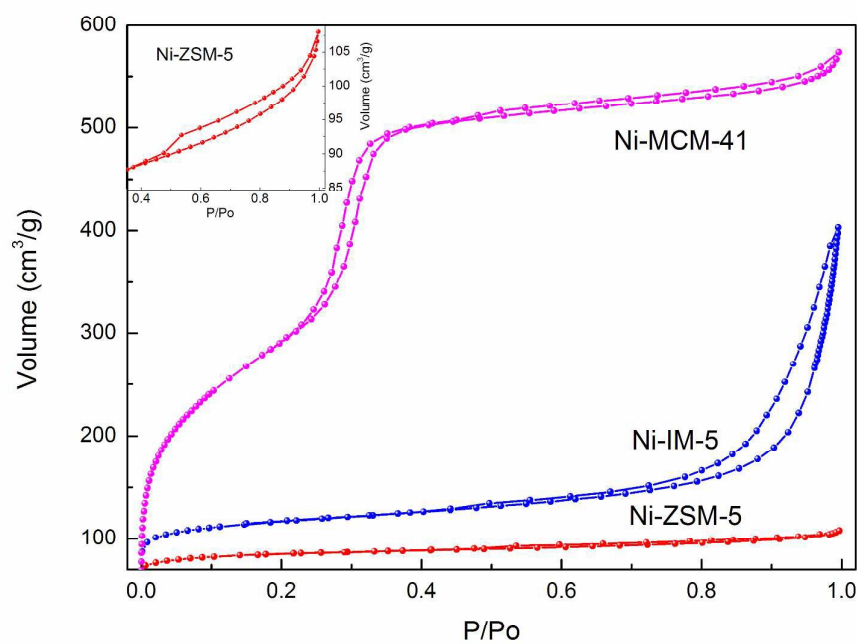


Fig. 1. Nitrogen adsorption–desorption isotherms of different Ni-modified catalysts

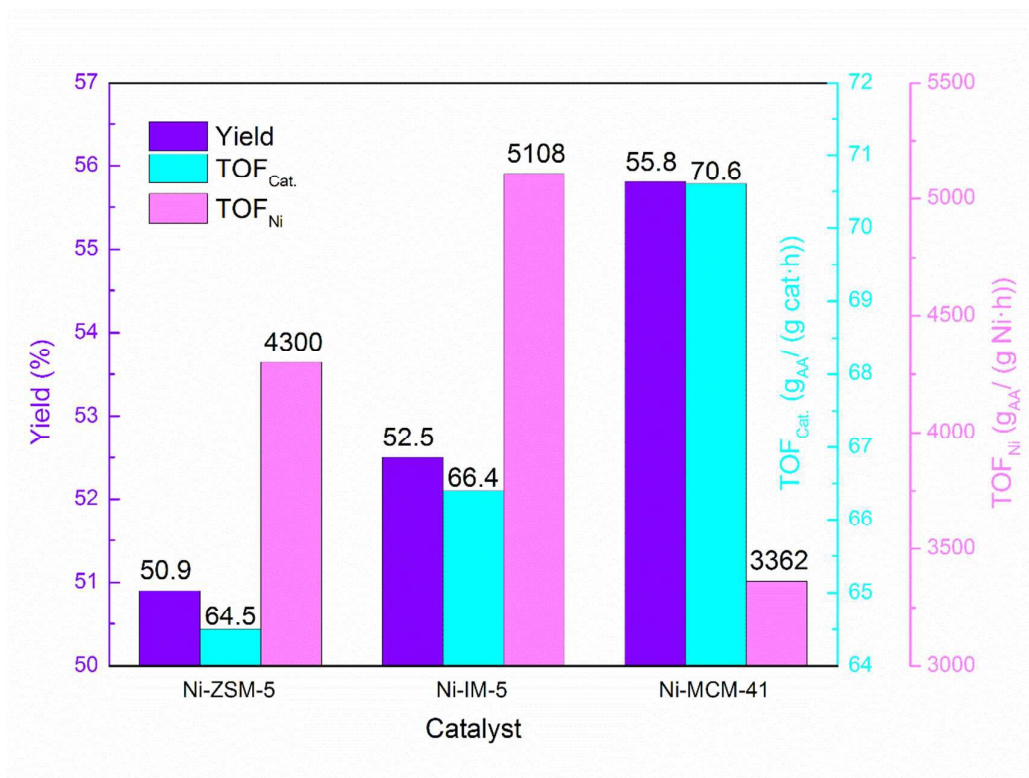


Fig. 2. The yield and TOF of the different Ni-modified catalysts

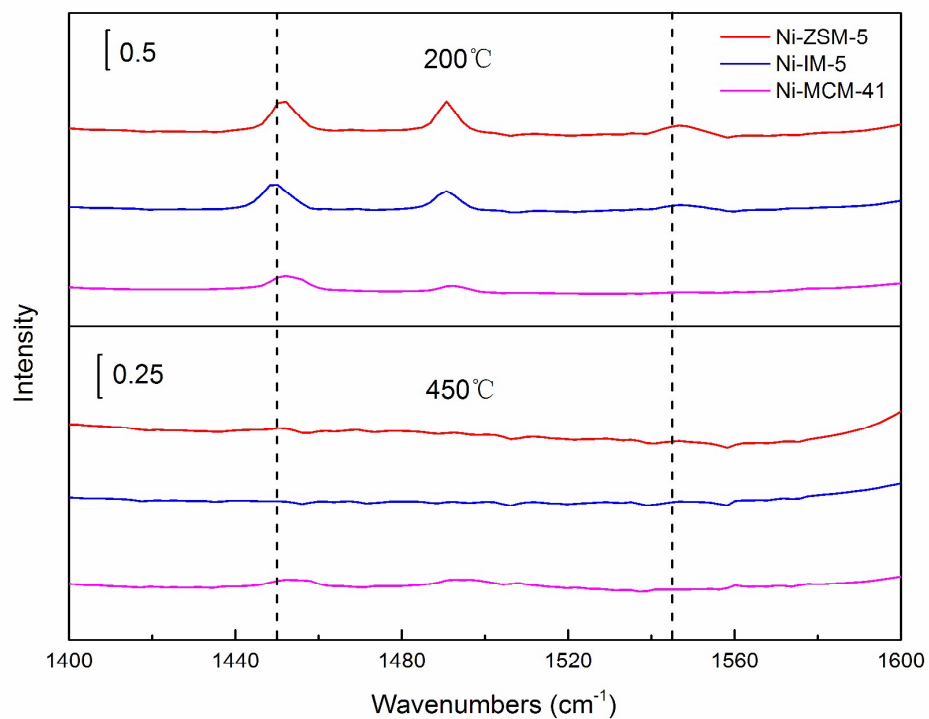


Fig. 3 Pyridine-FTIR spectra of the Ni-modified catalyst at 200°C and 450°C

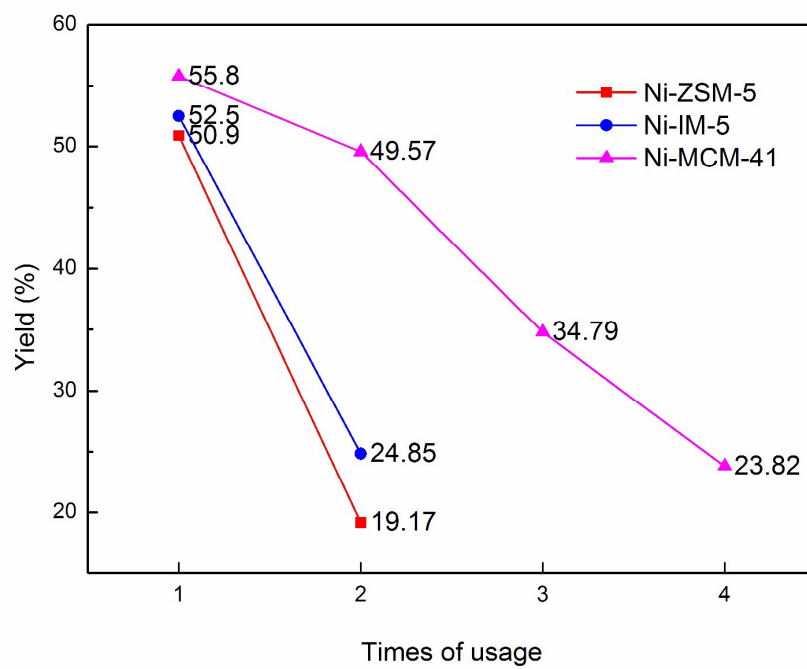


Fig. 4. Reusability test of Ni-modified catalysts

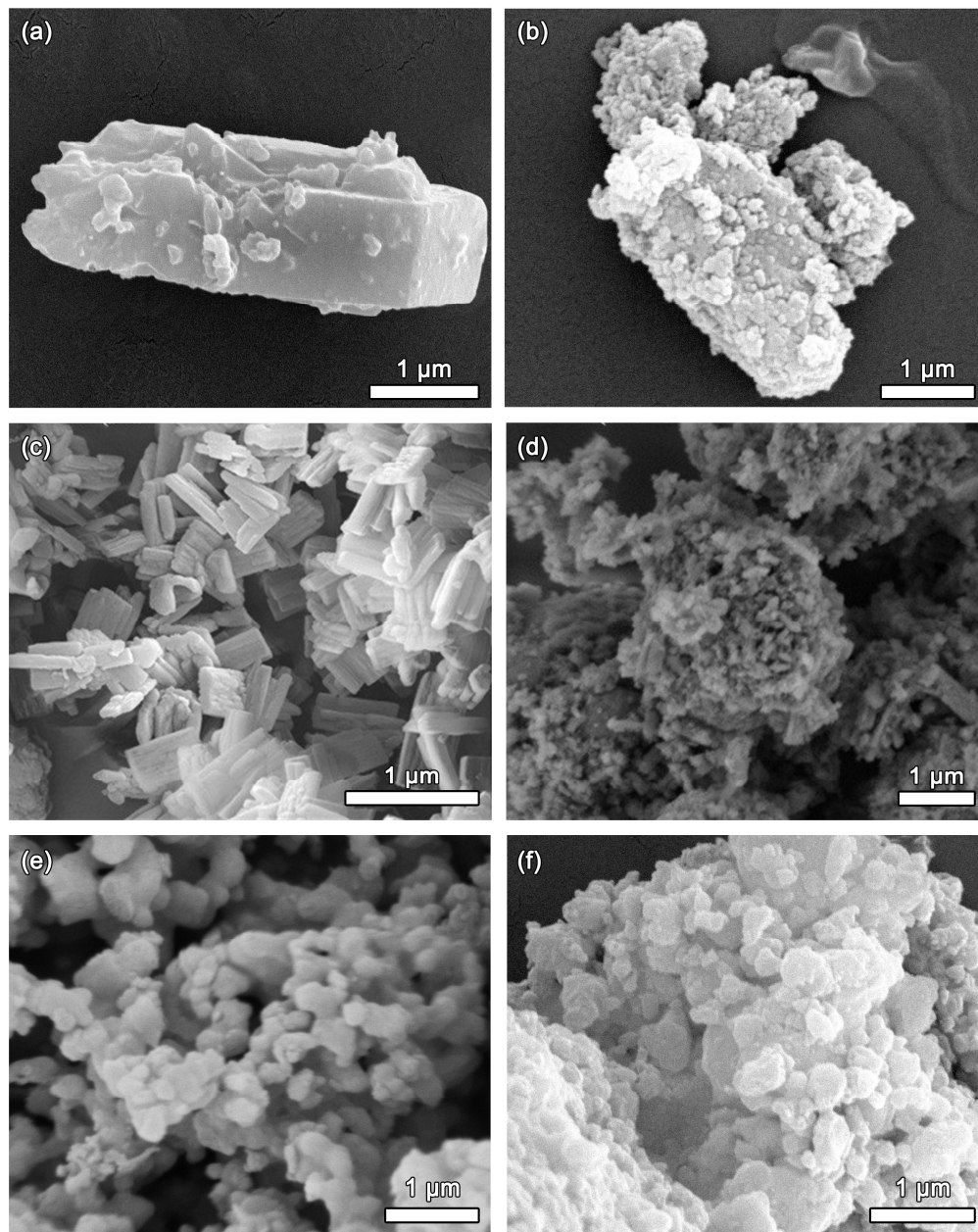


Fig. 5. SEM micrographs of fresh Ni-modified catalysts (a, Ni-ZSM-5, c, Ni-IM-5, e, Ni-MCM-41) and recovered Ni-modified catalysts (b, Ni-ZSM-5, d, Ni-IM-5, f, Ni-MCM-41)

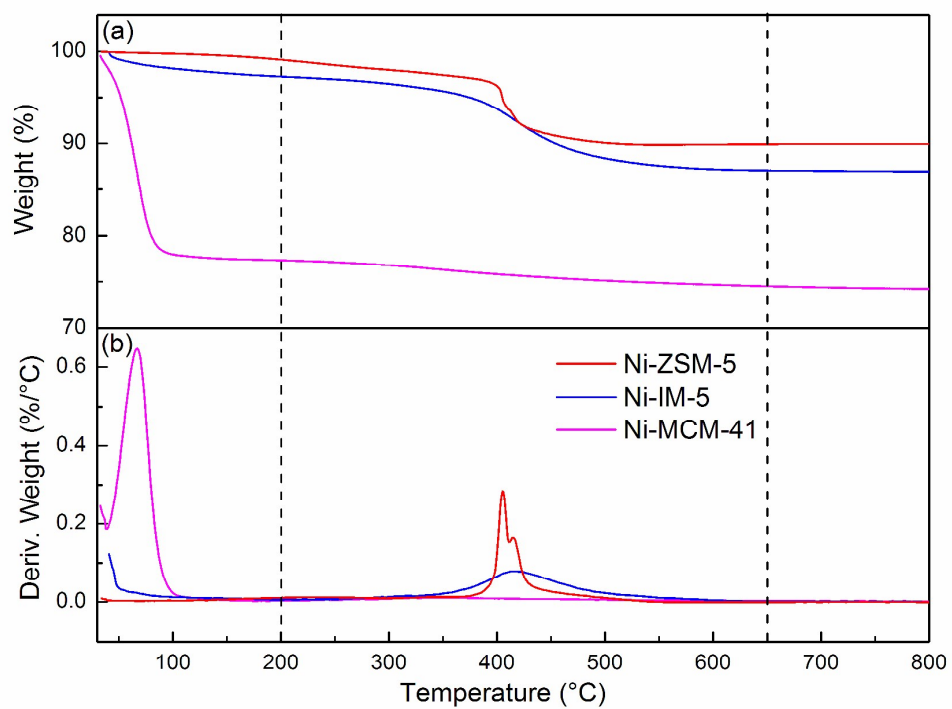


Fig. 6. Thermogravimetric analysis of the recovered Ni modified catalysts: (a) weight loss as function of temperature (TG) and (b) derivative weight loss as function of temperature (DTG).